# On the equivalence of nonequilibrium and equilibrium measurements of slip in molecular dynamics simulations

N. G. Hadjiconstantinou and M. M. Swisher◉
*Department of Mechanical Engineering, Massachusetts Institute of Technology,*
*Cambridge, Massachusetts 02139, USA*

We show that nonequilibrium and equilibrium measurements of slip are consistent, provided the hydrodynamic wall location associated with the equilibrium measurement is properly taken into account. The latter is a strong function of the fluid state and wall-fluid interaction and cannot be neglected as it typically has been. Our results are based on an alternative approach for calculating the hydrodynamic wall location which alleviates most of the difficulties associated with its calculation via a Green-Kubo integral that appear to have contributed to its neglect. Extensive molecular dynamics simulations are used to validate our approach including a model for calculating the slip length that does not involve a Green-Kubo integral.

## I. INTRODUCTION

The hydrodynamic behavior of fluids under confinement is a topic of significant theoretical and practical importance. In many instances, slip or jump boundary conditions can be used [1–3] to extend the range of validity of traditional macroscopic hydrodynamic models into the regime of small or in some cases even moderate confinement. The most-well-known boundary condition of this type is perhaps the Navier slip boundary condition

$$u_x|_{z=z^w} = \beta \frac{\partial u_x}{\partial z}\bigg|_{z=z^w}, \tag{1}$$

given here for a fluid-solid boundary, parallel to the $z = 0$ plane and located at $z = 0$; $z = z^w$ denotes the hydrodynamic wall location. We have also assumed, without loss of generality, that the solid boundary, or wall, is at rest and that the fluid flow and resulting slip are in the $x$ direction.

Reliable methods for calculating the slip length $\beta$ using molecular dynamics (MD) simulations are invaluable both from a practical point of view but also for informing fundamental research [4–11] into relation (1) based on a microscopic description of the fluid-solid interaction at their interface. Slip in MD simulations can be measured in the presence of a velocity gradient by extrapolating the velocity profile to the wall location. This approach is referred to as the nonequilibrium method. The inherent presence of nonequilibrium is considered to be a disadvantage by some authors, since, if the deviation from equilibrium is large, viscous heating, associated thermostats, or other nonlinear effects may contaminate the result. In response to this school of thought, methods for measuring slip using equilibrium simulations have also been developed. The most well known, perhaps, is the Green-Kubo method proposed by Bocquet and Barrat [5], which invokes linear response theory to calculate $\beta$. More recently, Duque-Zumajo *et al.* [12] developed an alternative approach which avoids the well-known plateau problem associated with the Green-Kubo (GK) formulation [12–14]. Interestingly, in one of their publications [13] they were able to show that their GK expressions,

although different in appearance, are equivalent to the original result of Bocquet and Barrat. Here we also note the work by Hansen *et al.* [15], who first introduced the concept of the near-wall fluid slab on which the analysis by Duque-Zumajo *et al.* is based.

Given the existence of these two quite different approaches to measuring slip in MD simulations, the lack of a comprehensive investigation into their equivalence is conspicuous by its absence. Comparisons between the two methods have been cursory, typically limited to the case of large slip length, with the hydrodynamic wall location, an important parameter within the GK method, neglected. On the other hand, typical modern computational resources are sufficient for performing low statistical uncertainty [16] nonequilibrium simulations at small deviations from equilibrium such that nonlinear effects are negligible. In this work we undertake this task, namely a detailed comparison between nonequilibrium and GK measurements of slip to show the that the two approaches are indeed equivalent, provided the hydrodynamic wall location is properly taken into account. To this effect we propose an alternative approach for determining the latter quantity. Additionally, by partially evaluating the GK relation for the slip length developed by Bocquet and Barrat, we develop a model for calculating the slip length that does not involve a GK integral.

## II. HYDRODYNAMIC WALL LOCATION VIA TANGENTIAL FORCE BALANCE AT THE WALL

We consider an atomic liquid in contact with an atomically smooth solid. Let $z$ denote the direction normal to the solid-liquid interface and pointing into the liquid, with $z = 0$ corresponding to the first layer of solid atoms in contact with the liquid.

According to the GK theory of Bocquet and Barrat [5], the slip length appearing in Eq. (1) can be calculated from

$$\beta_{\mathrm{GK}} = \frac{\mu A k_B T}{\int_0^\infty \langle F_x(t) F_x(0) \rangle dt}. \tag{2}$$

In this expression, angular brackets denote an ensemble average, $A$ denotes the interface area, $k_B$ is Boltzmann's constant, $\mu$ is the fluid viscosity, and $T$ is the (interface) temperature. Moreover $F_x(t)$ denotes the force exerted by the solid onto the fluid in the $x$ (slip) direction. According to this theory, the hydrodynamic wall location at which relation (1) is to be applied is not the fluid-solid interface ($z = 0$), but a location inside the fluid given by

$$z_{\mathrm{GK}}^w = \frac{\int_0^\infty \langle F_x(t) \Pi_{xz}(0) \rangle dt}{\int_0^\infty \langle F_x(t) F_x(0) \rangle dt}, \tag{3}$$

where $\Pi_{xz} = \sum_i m_i v_{xi} v_{zi} + \sum f_{xi} z_i$ defines the $x$-$z$ component of the fluid stress tensor, $v_{ji}$ denotes the velocity of atom $i$ in the direction $j$, and $m_i$ denotes the mass of atom $i$; $i$ runs through all liquid atoms. Here we note that $f_{xi}$, the $x$-direction component of the force on liquid atom $i$, includes the forces exerted by the solid onto the liquid.

A well-known issue [5] that limits the accuracy of GK approaches in finite systems (MD simulations) is associated with the identification of the plateau in integrals such as $\int_0^\infty \langle F_x(t) F_x(0) \rangle dt$. As remarked above, Dugue-Zumajo *et al.* recently proposed [14] a reformulation that avoids these theoretical difficulties. On the other hand, researchers using Eq. (2) typically sidestep this issue by approximating [5] the plateau with the first peak of $\int_0^t \langle F_x(t') F_x(0) \rangle dt'$. Oga *et al.* [17] recently provided some supporting argumentation for this approach by developing a model for the time evolution of $\langle F_x(t) F_x(0) \rangle$ which reduces calculation of the autocorrelation integral to the determination of three fitting coefficients in the model. Assuming their model to provide an accurate estimate of the GK integral, they showed that the error incurred by calculating $\beta_{\mathrm{GK}}$ using the first peak of the function $\int_0^t \langle F_x(t') F_x(0) \rangle dt'$ becomes small when the separation between the viscoelastic and GK relaxation timescales in the system studied is large; moreover, according to their model, for typical values of these timescales found in MD simulations the discrepancy is on the order of a few percent. Our MD results (see Fig. 1) are consistent with these findings, namely, identifying the
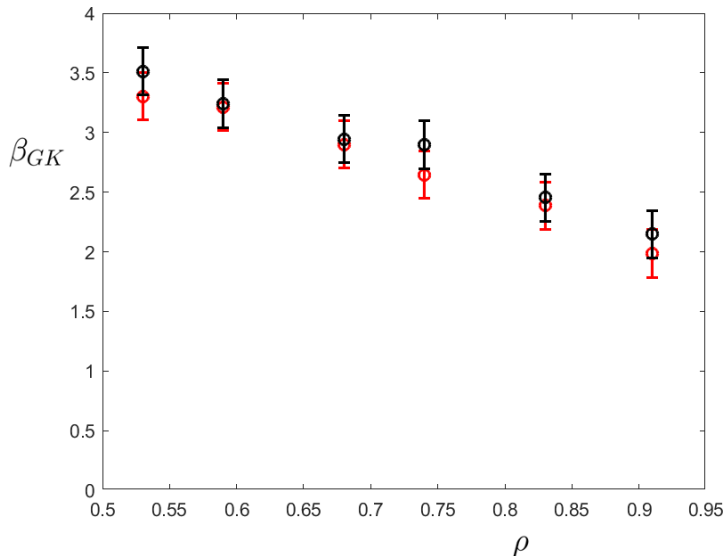
FIG. 1. Comparison between estimates of $\beta_{GK}$ calculated using the model of Oga *et al.* [17] (red) and by identifying the plateau by the first maximum of the running integral $\int_0^t \langle F_x(t')F_x(0)\rangle dt'$ (black). Simulations were performed at $T = 1.5$ for $\varepsilon_{sl} = 1$ and $C_{sl} = 0.6$.

plateau with the first peak of $\int_0^t \langle F_x(t')F_x(0)\rangle dt'$ results in a small overestimation of $\beta_{GK}$ of order 5% compared to the value predicted by the model of Oga *et al.*

Evaluation of the expression (3) is more challenging. In addition to being significantly more sensitive to noise [5] than (2), a reliable approach for identifying the plateau in the additional GK integral is yet to be developed. As a result, the hydrodynamic wall location has received considerably less attention, with studies utilizing the GK formulation simply ignoring its existence or perhaps implicitly assuming that it is small compared to the slip length. Unfortunately, as will be seen below, the latter is not an appropriate assumption, even in the case of moderately large slip length. This can perhaps be used to explain the existence of a number of publications questioning the validity of (2); the reader is referred to Ref. [12] for a more thorough review of this body of work.

Our objective here is to perform a thorough validation of the GK approach by comparing its predictions to nonequilibrium measurements of slip. To achieve this goal we need accurate measurements of the hydrodynamic wall location. We obtain those by using the tangential force balance at the wall [5]

$$\langle F_x \rangle = -\mu A \frac{u_x(z = z_{GK}^w)}{\beta_{GK}}. \tag{4}$$

This serves as an implicit equation for $z_{GK}^w$, since the slip velocity $u_x(z = z_{GK}^w)$ involves the (hydrodynamic) wall location in its definition. In other words, given a measurement of the force on the solid boundary, $z_{GK}^w$ can be determined as the location at which $u_x(z = z_{GK}^w)$ satisfies (4), with $\beta_{GK}$ determined from Eq. (2).

## III. VALIDATION

We have performed equilibrium and nonequilibrium MD simulations of a model system over a variety of conditions in order to (a) validate the ability of Eq. (4) to determine the hydrodynamic wall location and (b) make a comprehensive comparison between equilibrium and nonequilibrium measurements of slip. Our simulations were performed using the LAMMPS software [18]. The model system, simulation setup, and parameters as well as our results are described in detail below.

### A. Molecular simulation setup

We consider a system comprising a dense liquid bounded by two fcc-structured walls in a slab geometry. Atomic interactions follow the generalized Lennard-Jones (LJ) potential [19]

$$u_{ij}(r) = 4\varepsilon_{ij}\left[\left(\frac{\sigma_{ij}}{r}\right)^{12} - C_{ij}\left(\frac{\sigma_{ij}}{r}\right)^{6}\right], \tag{5}$$

where $r$ denotes the distance between atoms $i$ and $j$.

In what follows, we will use subscript $s$ to denote solid atoms and their properties and $l$ to denote liquid atoms and their properties. All quantities will be reported in nondimensional units using the characteristic time $\tau_{LJ} = \sqrt{m_l\sigma_{ll}^2/\varepsilon_{ll}}$, the characteristic distance $\sigma_{ll}$, and the potential well depth $\varepsilon_{ll}$ associated with the liquid-liquid interaction. In all our simulations $C_{ss} = C_{ll} = 1$, while $C_{sl}$ was varied in the range $0.4 \leqslant C_{sl} \leqslant 1$ as will be discussed below.

The simulated system measured 30.8 LJ units in each of the two dimensions parallel to the walls; the distance between the walls was also $L = 30.8$ units. Increasing $L$ to 61.6 units did not produce any significant change in our results.

Each wall consisted of a 7.71-unit-thick fcc slab of atoms divided into three regions, each under different dynamics. The outermost region contained three atomic layers frozen in place. The middle region contained seven atomic layers thermostated to the desired system temperature $T$ via a Nosé-Hoover thermostat. The innermost region, in contact with the fluid, comprised of a single atomic layer under $NVE$ dynamics. The surface of the wall exposed to the fluid is the (0,0,1) plane of the fcc crystal. The wall density was fixed at $n_w = 1.09$. In all simulations $m_s = 5$ ($m_l = 1$), $\sigma_{sl} = 1$ ($\sigma_{ll} = 1$), and $\varepsilon_{ss} = 4$ ($\varepsilon_{ll} = 1$). A potential cutoff of 5 LJ units was used.

#### 1. Equilibrium simulations

We calculate $\beta_{GK}$ by numerical integration of the wall-force autocorrelation trace, namely, inserting the result for $\int_0^\infty \langle F_x(t)F_x(0)\rangle dt$ into (2). In all results presented here, the plateau value of $\int_0^\infty \langle F_x(t)F_x(0)\rangle dt$ is identified with the maximum value of this function, in accordance with our discussion in Sec. II.

#### 2. Nonequilibrium simulations

We performed Couette flow simulations at wall speeds of $\pm 0.1$, which are sufficiently small for nonlinear effects to be negligible and viscous heating to be small (maximum temperature variation across the fluid was less than 0.01). The nonequilibrium slip length, denoted by $\beta_{neq}$, was defined as the distance into the wall at which the extrapolated fluid velocity profile reaches the wall speed value. The above extrapolation was performed via a linear approximation of the velocity profile fitted over the middle 75% of the fluid domain, away from the layering present close to the walls [20].

Here we note that the slip length obtained by this procedure implicitly assumes that the hydrodynamic wall location is $z = 0$ ($z_{neq}^w = 0$). As will be seen below, this leads to considerable differences between the equilibrium and nonequilibrium results for the slip length. The two can be compared by referring both to the same hydrodynamic wall location. In the present case, this was done by referring the nonequilibrium value to the GK hydrodynamic wall location, or in other words by comparing $\beta_{GK}$ to $\beta_{neq} + z_{GK}^w$, where $z_{GK}^w$ was determined using Eq. (4). We note that due to the linear velocity profile in Couette flow, this convention is arbitrary: Comparing $\beta_{GK} - z_{GK}^w$ to $\beta_{neq}$ is equivalent.

### B. Simulation results

Simulations were performed for a wide variety of conditions, including variable liquid density, variable temperature, variable solid-liquid attraction as characterized by $C_{sl}$, and variable liquid-sold interaction strength. Figures 2–6 show comparisons between the slip length as determined
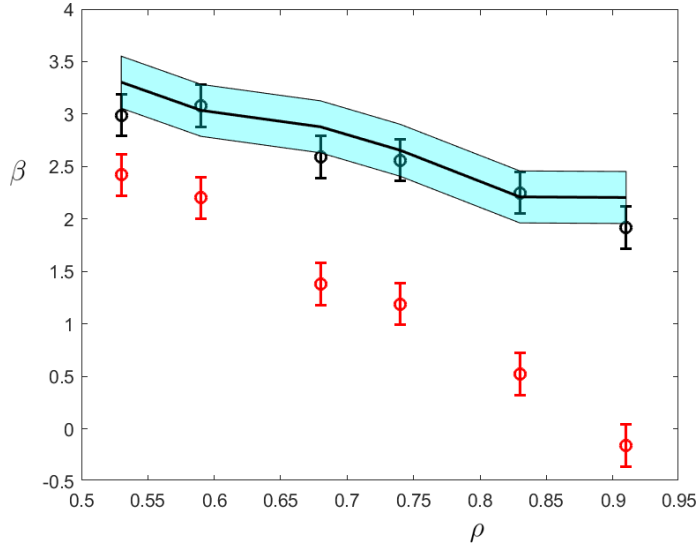
FIG. 2. Comparison between the Green-Kubo prediction $\beta_{\text{GK}}$ and the nonequilibrium slip $\beta_{\text{neq}}$ as a function of fluid density at $T = 1.5$ with $\varepsilon_{sl} = 1$ and $C_{sl} = 0.6$. Red symbols denote $\beta_{\text{neq}}$ at $z = 0$ and black symbols denote $\beta_{\text{neq}}$ referred to $z = z_{\text{GK}}^w$ ($\beta_{\text{neq}} + z_{\text{GK}}^w$); the predictions and uncertainty associated with $\beta_{\text{GK}}$ are shown by the black line and blue shading, respectively.

from Eq. (2) via equilibrium simulations ($\beta_{\text{GK}}$), the slip length as determined by nonequilibrium simulations ($\beta_{\text{neq}}$), and the nonequilibrium slip length referred to $z = z_{\text{GK}}^w$ ($\beta_{\text{neq}} + z_{\text{GK}}^w$). Each data point corresponds to the average value of the results from each of the two walls in the system. In these comparisons, Eq. (2) was evaluated using bulk fluid properties. The results clearly establish
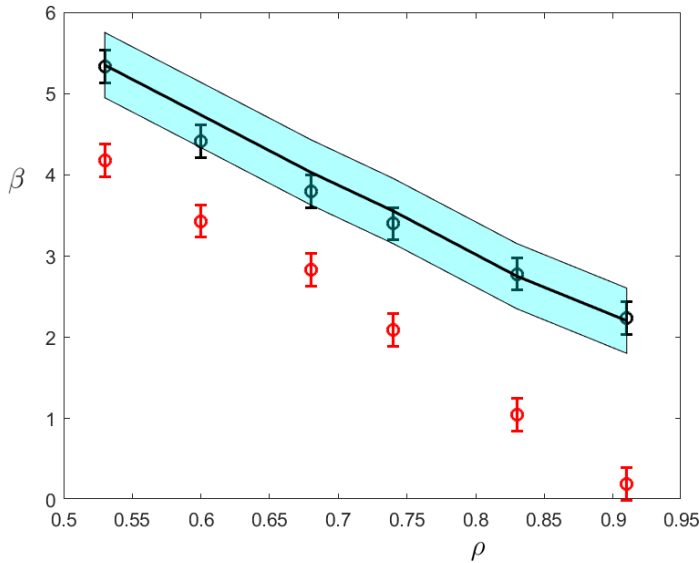


FIG. 3. Comparison between the Green-Kubo prediction $\beta_{\text{GK}}$ and the nonequilibrium slip $\beta_{\text{neq}}$ as a function of fluid density at $T = 1.5$ with $\varepsilon_{sl} = 0.6$ and $C_{sl} = 0.6$. Red symbols denote $\beta_{\text{neq}}$ at $z = 0$ and black symbols denote $\beta_{\text{neq}}$ referred to $z = z_{\text{GK}}^w$ ($\beta_{\text{neq}} + z_{\text{GK}}^w$); the predictions and uncertainty associated with $\beta_{\text{GK}}$ are shown by the black line and blue shading, respectively.
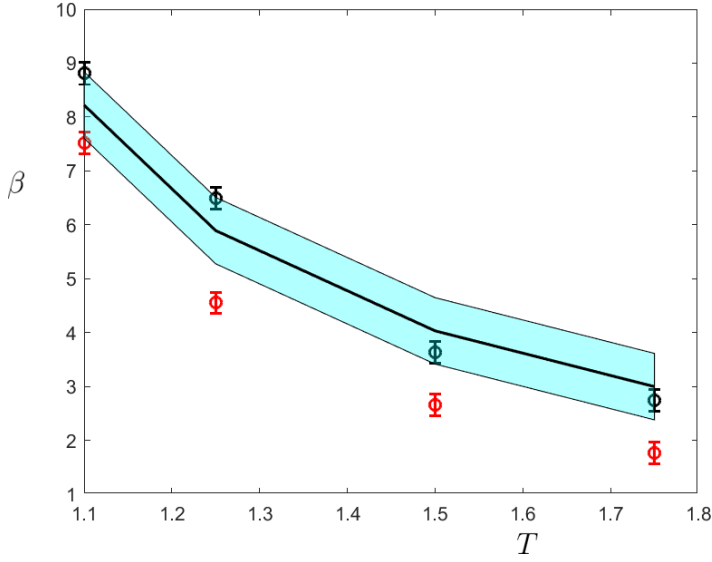
FIG. 4. Comparison between the Green-Kubo prediction $\beta_{\mathrm{GK}}$ and the nonequilibrium slip $\beta_{\mathrm{neq}}$ as a function of temperature at $\rho = 0.68$ with $\varepsilon_{sl} = 0.6$ and $C_{sl} = 0.6$. Red symbols denote $\beta_{\mathrm{neq}}$ at $z = 0$ and black symbols denote $\beta_{\mathrm{neq}}$ referred to $z = z_{\mathrm{GK}}^{w}$ ($\beta_{\mathrm{neq}} + z_{\mathrm{GK}}^{w}$); the predictions and uncertainty associated with $\beta_{\mathrm{GK}}$ are shown by the black line and blue shading, respectively.

that nonequilibrium measurements of the slip length at the fluid-solid interface, that is, without taking into account the hydrodynamic wall location, can be very different from those predicted by the GK theory (2). However, when the hydrodynamic wall location is taken into account, in the present figures by referring the nonequilibrium result to this location, the agreement between the two
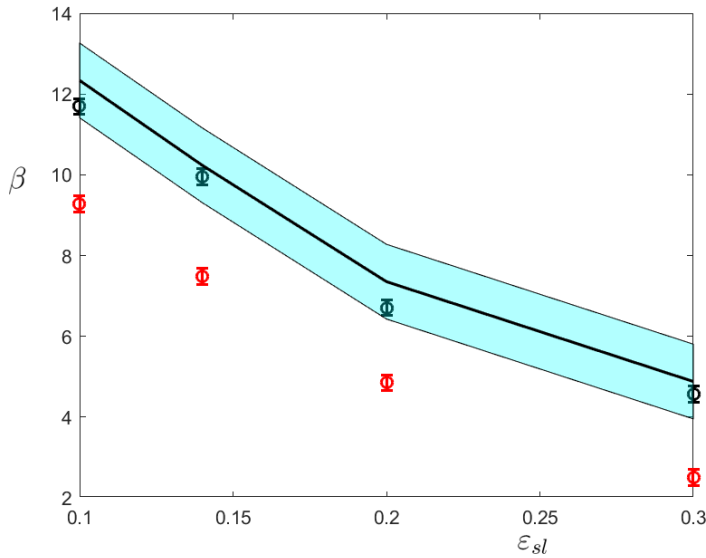


FIG. 5. Comparison between the Green-Kubo prediction $\beta_{\mathrm{GK}}$ and the nonequilibrium slip $\beta_{\mathrm{neq}}$ as a function of $\varepsilon_{sl}$ at $T = 0.825$ and $\rho = 0.83$ with $C_{sl} = 1$. Red symbols denote $\beta_{\mathrm{neq}}$ at $z = 0$ and black symbols denote $\beta_{\mathrm{neq}}$ referred to $z = z_{\mathrm{GK}}^{w}$ ($\beta_{\mathrm{neq}} + z_{\mathrm{GK}}^{w}$); the predictions and uncertainty associated with $\beta_{\mathrm{GK}}$ are shown by the black line and blue shading, respectively.
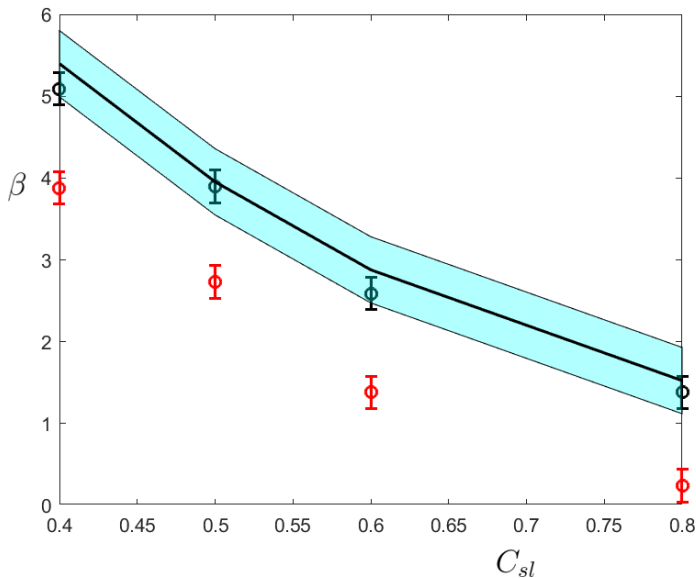
FIG. 6. Comparison between the Green-Kubo prediction $\beta_{\mathrm{GK}}$ and the nonequilibrium slip $\beta_{\mathrm{neq}}$ as a function of $C_{\mathrm{sl}}$ at $T = 1.5$ and $\rho = 0.68$ with $\varepsilon_{sl} = 1$. Red symbols denote $\beta_{\mathrm{neq}}$ at $z = 0$ and blue symbols denote $\beta_{\mathrm{neq}}$ referred to $z = z_{\mathrm{GK}}^w$ ($\beta_{\mathrm{neq}} + z_{\mathrm{GK}}^w$); the predictions and uncertainty associated with $\beta_{\mathrm{GK}}$ are shown by the black line and blue shading, respectively.

methods is excellent. This also serves as a validation of using (4) to determine the hydrodynamic wall location.

These results also show that the magnitude of $z_{\mathrm{GK}}^w$ can be significantly larger than the value of one LJ unit usually assumed in the literature and as such it cannot be neglected, especially since it appears to be sensitive to the fluid state.

## IV. EXPRESSION FOR $\beta$ WHICH DOES NOT INVOLVE A GK INTEGRAL

In this section we discuss a model for calculating $\beta$ without evaluating a GK integral. This result is inspired by previous work [6], where such an expression was developed by relating the force autocorrelation integral in (2) to a model for the relaxation dynamics of the density-density correlation function, using a number of approximations as well as a detailed account of fluid-solid interaction dynamics. The present work also models the force autocorrelation integral but follows a different route, based on the observation, first reported for the case of the Kapitza resistance [21], that the timescale associated with the GK integral governing interfacial transport can be approximately estimated using bulk fluid transport properties. This observation enables the elimination of the autocorrelation integral in terms of the mean square of the tangential component of the wall-fluid force and known fluid properties, arguably resulting in a simpler and more physically intuitive final expression.

Following [21], we write (2) in the form

$$\beta = \frac{\mu A k_B T}{\langle F_x^2 \rangle \int_0^\infty \phi(t) dt} = \frac{\mu A k_B T}{\langle F_x^2 \rangle I_\beta}, \tag{6}$$

where $\phi(t) = \langle F_x(t) F_x(0) \rangle / \langle F_x^2 \rangle$ and

$$I_\beta = \lim_{t \to \infty} \int_0^t \phi(t') dt'. \tag{7}$$

The importance of this rearrangement is that it reduces the contribution of the GK integral in (2) into the two distinct factors, namely, $\langle F_x^2 \rangle$, which is strongly dependent on the fluid-solid interaction and fluid state, and the timescale $I_\beta$, which our MD simulations show, in agreement with the results in [21] for the case of the Kapitza resistance, is a very weak function of the fluid state and fluid-solid interaction. Further progress can be made by introducing the assumption $I_\beta = \tau / D_\beta$, where $D_\beta$ is a constant and $\tau$ is the homogeneous fluid relaxation timescale defined by

$$\mu = \frac{1}{V k_B T} \int_0^\infty \langle \Pi_{ij}(t) \Pi_{ij}(0) \rangle dt = \frac{\langle \Pi_{ij}^2 \rangle}{V k_B T} \int_0^\infty \frac{\langle \Pi_{ij}(t) \Pi_{ij}(0) \rangle}{\langle \Pi_{ij}^2 \rangle} dt = G_\infty \tau, \qquad (8)$$

where $\Pi_{ij}$ denotes a nondiagonal component of the homogeneous fluid stress tensor ($i \neq j$) and

$$G_\infty = \frac{1}{V k_B T} \langle \Pi_{ij}^2 \rangle \qquad (9)$$

is the fluid high-frequency shear modulus [22]. This assumption yields

$$\beta = \frac{D_\beta G_\infty k_B T}{A^{-1} \langle F_x^2 \rangle}, \qquad (10)$$

in which the dynamics hidden within the GK integral have been expressed in terms of system properties.

Figure 7 shows that Eq. (10) provides a very reasonable approximation to our MD results. In this comparison, the value $D_\beta = 1.05$ was chosen as the one that gives best overall agreement between the expression (10) and the MD results; $G_\infty$ was calculated using the analytical expression for a LJ potential in [23], while $A^{-1} \langle F_x^2 \rangle$ was taken from MD simulations. Here we emphasize that once determined as described above, the value of $D_\beta$ is not adjusted in any way; this is quite remarkable given the variety of fluid conditions and solid-liquid interaction parameters explored in this figure.

## V. DISCUSSION

We have shown that nonequilibrium and equilibrium measurements of slip are consistent, provided the hydrodynamic wall location associated with the equilibrium measurement is taken into account. Moreover, our simulations showed that the hydrodynamic wall location associated with $\beta_{GK}$ is dependent on the fluid state in a nontrivial manner and can be a significant fraction of the slip length. In other words, $z_{GK}^w$ cannot be neglected in general; instead, a reliable method for its calculation is needed. Our work has shown that reliable and accurate measurements of $z_{GK}^w$ can be obtained by utilizing the tangential force balance at the wall in a nonequilibrium shear flow, given by Eq. (4). Given that the latter approach requires a nonequilibrium simulation, we note here that a method which uses MD simulations of two nonequilibrium flows, namely, a Couette and a Poiseuille flow, to calculate the slip length and the associated hydrodynamic wall location was recently proposed in [24]. The need for two distinct simulations for simultaneously determining both of these quantities was first discussed in [5]; a variant of this approach was implemented for dissipative particle dynamics simulations in [25]. A comparison between the method proposed here and the one that uses two nonequilibrium simulations would be an interesting topic for future work.

The relative success of the approximation $I_\beta = \tau / D_\beta$ is also worth noting because it enables the closed-form expression (10) and also because the similar success of the analogous approximation in the case of the Kapitza resistance [21] suggests some generality. Models such as Eq. (10) as well as others [6,9] are valuable because they replace the GK integral with a more transparent connection between system properties and the slip length. Returning to (10), further work is required for developing methodologies for calculating the value of $D_\beta$ from first principles. We also note that, based on our results, relation (10) would benefit from a model for predicting the associated hydrodynamic wall location; this is a subject left for future work.
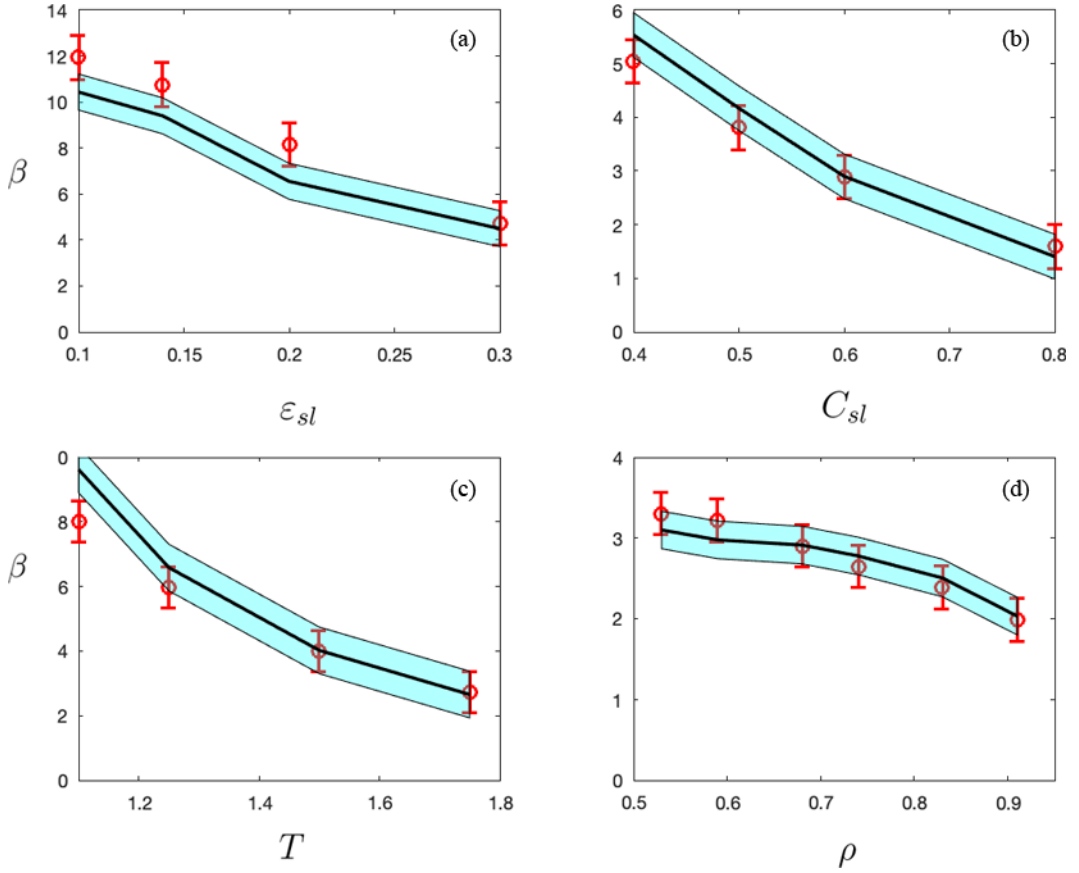
FIG. 7. Validation of relation (10) for a variety of conditions. Molecular dynamics simulation results and associated uncertainty (for $\beta_{GK}$) are shown by red symbols, while the prediction of Eq. (10) and associated uncertainty are denoted by the black line and blue shading, respectively. Simulations were performed at the following conditions: (a) $T = 0.825$, $C_{sl} = 1$, and $\rho = 0.83$; (b) $T = 1.5$, $\varepsilon_{sl} = 1$, and $\rho = 0.68$; (c) $\varepsilon_{sl} = 0.6$, $C_{sl} = 0.6$, and $\rho = 0.68$; and (d) $T = 1.5$, $\varepsilon_{sl} = 1$, and $C_{sl} = 0.6$.

The new GK formulation by de la Torre *et al.* [12,13], aimed at alleviating the GK plateau issue discussed in Sec. II, also introduced a modified hydrodynamic wall location $z_{GK}^{w,C} = z_{GK}^{w} - G\beta_{GK}/\mu$, where $G > 0$, given in terms of a GK integral, represents a correction to the fluid viscosity at this location due to the wall presence [26]. Provided the evaluation of $G$ is less challenging than that of $z_{GK}^{w}$, this new formulation may indeed be preferable, since it could provide less ambiguous estimates of $\beta_{GK}$ coupled to a smaller in magnitude, and thus less important compared to the slip value, hydrodynamic wall location. Such a formulation would also be advantageous for models such as the one presented in Sec. IV, since it diminishes the importance of accurately determining $z_{GK}^{w,C}$ (or $z_{GK}^{w}$).

[1] *Molecular Gas Dynamics: Theory, Techniques, and Applications*, edited by Y. Sone (Birkhäuser, Boston, 2007).

[2] N. G. Hadjiconstantinou, The limits of Navier-Stokes theory and kinetic extensions for describing small-scale gaseous hydrodynamics, Phys. Fluids **18**, 111301 (2006).

[3] N. Kavokine, R. R. Netz, and L. Bocquet, Fluids at the nanoscale: From continuum to subcontinuum transport, Annu. Rev. Fluid Mech. **53**, 377 (2021).

[4] P. A. Thompson and S. M. Troian, A general boundary condition for liquid flow at solid surfaces, Nature (London) **389**, 360 (1997).

[5] L. Bocquet and J.-L. Barrat, Hydrodynamic boundary conditions, correlation functions, and Kubo relations for confined fluids, Phys. Rev. E **49**, 3079 (1994).

[6] J. L. Barrat and L. Bocquet, Influence of wetting properties on hydrodynamic boundary conditions at a fluid/solid interface, Faraday Discuss. **112**, 119 (1999).

[7] S. Lichter, A. Roxin, and S. Mandre, Mechanisms for Liquid Slip at Solid Surfaces, Phys. Rev. Lett. **93**, 086001 (2004).

[8] A. Martini, A. Roxin, R. Q. Snurr, Q. Wang, and S. Lichter, Molecular mechanisms of liquid slip, J. Fluid Mech. **600**, 257 (2008).

[9] N. V. Priezjev and S. M. Troian, Influence of periodic wall roughness on the slip behavior at liquid/solid interfaces: Molecular scale simulations versus continuum predictions, J. Fluid Mech. **554**, 25 (2006).

[10] G. J. Wang and N. G. Hadjiconstantinou, Universal molecular-kinetic scaling relation for slip of a simple fluid at a solid boundary, Phys. Rev. Fluids **4**, 064201 (2019).

[11] N. G. Hadjiconstantinou, An atomistic model for the Navier slip condition, J. Fluid Mech. **912**, A26 (2021).

[12] D. Duque-Zumajo, J. A. de la Torre, D. Camargo, and P. Español, Discrete hydrodynamics near solid walls: Non-Markovian effects and the slip boundary condition, Phys. Rev. E **100**, 062133 (2019).

[13] D. Camargo, J. A. de la Torre, R. Delgado-Buscalioni, F. Chejne, and P. Español, Boundary conditions derived from a microscopic theory of hydrodynamics near solids, J. Chem. Phys. **150**, 144104 (2019).

[14] J. A. de la Torre, D. Duque-Zumajo, D. Camargo, and P. Español, Microscopic Slip Boundary Conditions in Unsteady Fluid Flows, Phys. Rev. Lett. **123**, 264501 (2019).

[15] J. S. Hansen, B. D. Todd, and P. J. Daivis, Prediction of fluid velocity slip at solid surfaces, Phys. Rev. E **84**, 016313 (2011).

[16] N. G. Hadjiconstantinou, A. L. Garcia, M. Z. Bazant, and G. He, Statistical error in particle simulations of hydrodynamic phenomena, J. Comput. Phys. **187**, 274 (2003).

[17] H. Oga, Y. Yamaguchi, T. Omori, S. Merabia, and L. Joly, Green-Kubo measurement of liquid-solid friction in finite-size systems, J. Chem. Phys. **151**, 054502 (2019).

[18] S. Plimpton, Fast parallel algorithms for short-range molecular dynamics, J. Comput. Phys. **117**, 1 (1995).

[19] S. Alosious, S. K. Kannam, S. P. Sathian, and B. D. Todd, Prediction of Kapitza resistance at fluid-solid interfaces, J. Chem. Phys. **151**, 194502 (2019).

[20] G. J. Wang and N. G. Hadjiconstantinou, Molecular mechanics and structure of the fluid-solid interface in simple fluids, Phys. Rev. Fluids **2**, 094201 (2017).

[21] N. G. Hadjiconstantinou and M. M. Swisher, An atomistic model for the thermal resistance of a fluid-solid interface, J. Fluid Mech. **934**, R2 (2022).

[22] D. M. Heyes, D. Dini, L. Costigliola, and J. C. Dyre, Transport coefficients of the Lennard-Jones fluid close to the freezing line, J. Chem. Phys. **151**, 204502 (2019).

[23] R. Zwanzig and R. D. Mountain, High-frequency elastic moduli of simple fluids, J. Chem. Phys. **43**, 4464 (1965).

[24] H. Nakano and S. I. Sasa, Equilibrium measurement method of slip length based on fluctuating hydrodynamics, Phys. Rev. E **101**, 033109 (2020).

[25] J. Smiatek, M. P. Allen, and F. Schmid, Tunable-slip boundaries for coarse-grained simulations of fluid flow, Eur. Phys. J. E **26**, 115 (2008).

[26] P. Español (private communication).